ChemComm

COMMUNICATION

View Article Online
View Journal | View Issue

Cite this: *Chem. Commun.*, 2015, **51**, 12197

Received 1st June 2015,
Accepted 24th June 2015

DOI: 10.1039/c5cc04476f

www.rsc.org/chemcomm

In situ production of silver nanoparticles on an aldehyde-equipped conjugated porous polymer and subsequent heterogeneous reduction of aromatic nitro groups at room temperature†

Jie Liu,[a] Jieshun Cui,[a] Filipe Vilela,*[b] Jun He,[c] Matthias Zeller,[d] Allen D. Hunter[d] and Zhengtao Xu*[a]

In a metal-free procedure, chelating thiol groups and an electrophile react to assemble a robust, conjugated porous polymer with pendant aldehyde functionalities. These groups are able to reduce Ag(I) ions to generate, *in situ*, Ag(0) nanoparticles evenly dispersed in the polymer matrix. The Ag(0)–polymer composite enables selective reduction of aromatic nitro compounds as a heterogeneous catalyst, and can be conveniently recycled multiple times.

Anthropogenic climate change as a result of our current energy demands is of great concern in today's society. The need for new sources of clean and renewable energy alongside improved sustainable chemical processes has been the driving force behind the development of new materials. Conjugated porous polymers, (CPPs) as a growing class of advanced organic materials have received much attention due to their facile synthesis, low cost, and flexible chemical functionality. As the synthetic principles and structural studies continue to be extensively investigated, emphasis is being shifted to the properties and applications of these systems as novel organic zeolites. They have shown excellent performance in areas such as gas storage[1] and separation,[1d] by virtue of their high surface areas and porosity; metal-binding with high selectivities;[2] and heterogeneous catalysis[3] including photocatalysis.[4] Furthermore, the combination of metal-binding ability with heterogeneous catalysis has the potential to develop materials with enhanced catalytic activity. Although underexplored, there are a few examples of this strategy.[5]

CPPs loaded with metal nanoparticles have also proven to be an efficient method in the development of novel heterogeneous photocatalysts. A conjugated microporous polymer was reported to photocatalyse Suzuki–Miyaura cross-coupling reactions when loaded with Pd nanoparticles.[6] Li *et al.* also reported that mesoporous g-C_3N_4, can be used as photoactive anchoring support for Pd nanoparticles to perform the same chemical transformations.[7] These systems rely on the mixing of the CPP with a solution of nanoparticles leading to a cumbersome and wasteful process. By comparison, and to the best of our knowledge, there have been very few reports on nanoparticle synthesis *in situ* directly within a CPP network.[8]

Herein, we report a novel aldehyde-equipped porous polymer that can be easily synthesized in the absence of any metal catalyst, and can then be further post-modified to incorporate Ag nanoparticles (Ag NPs) *via* the use of Tollens' reagent. Our strategy allows for *in situ* formation of the Ag nanoparticles leading to a stable hybrid material that can be employed as a heterogeneous catalyst for the reduction of aromatic nitro compounds at room temperature. This application is particularly relevant to the pharmaceutical and agrochemical industries since synthesis of anilines or amines from the corresponding nitro compounds lead to versatile intermediates and precursors in the preparation of dyes, pharmaceuticals, pigments, agrochemicals and polymers.[9]

CPPs are generally synthesized *via* metal catalyzed coupling reactions. Typically these include Suzuki–Miyaura,[10] Sonogashira–Hagihara,[11] Yamamoto and Glaser polycondensations.[12] Other strategies such as oxidative polymerizations also rely on metals (typically $FeCl_3$).[13] Recently we reported a metal-free polymerization method simply by mixing two monomers in the presence of a mild base *N*,*N*′-diisopropylethylamine (DIPEA) that promoted C–N bond formation to produce a porous polymer framework in high yield.[2]

With regards to the synthesis of an aldehyde-equipped CPP, DIPEA was again employed to promote C–S bond formation *via* the use of a rigid monomer containing multiple chelating sites, triphenylene-2,3,6,7,10,11-hexathiol (HTT) (Scheme 1).

---

[a] *Department of Biology and Chemistry, City University of Hong Kong, 83 Tat Chee Avenue, Kowloon, Hong Kong, China. E-mail: zhengtao@cityu.edu.hk*
[b] *School of Engineering and Physical Sciences, Heriot-Watt University, Edinburgh, EH14 4AS, UK. E-mail: f.vilela@hw.ac.uk*
[c] *School of Chemical Engineering and Light Industry, Guangdong University of Technology, Guangzhou 510006, Guangzhou, China*
[d] *Youngstown State University, One University Plaza, Youngstown, Ohio 44555, USA*

† Electronic supplementary information (ESI) available: Experimental procedures; network synthesis; elemental analysis, N_2 and CO_2 sorption, TGA, IR, NMR, and PXRD data. CCDC 1401125. For ESI and crystallographic data in CIF or other electronic format see DOI: 10.1039/c5cc04476f

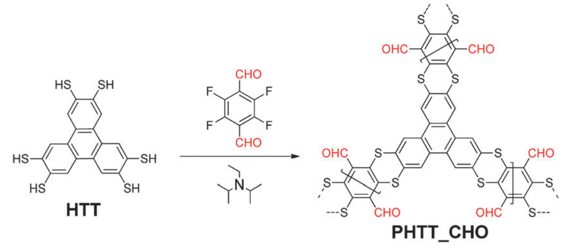

Scheme 1 Synthesis of the aldehyde-equipped CPP PHTT_CHO. Conditions: dimethylacetamide (DMA), DIPEA, N_2, 90 °C, 3 hours, then 140 °C, 12 hours.

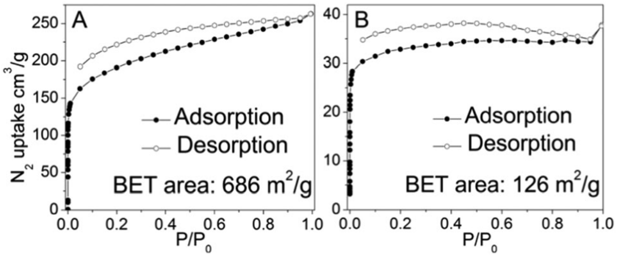

Fig. 1 N_2 sorption isotherms at 77 K for the activated solid samples of PHTT_CHO (A) and PHTT_Ag (B).

This methodology offers great advantages: the most important being the absence of any metal catalysts. In general, thiols can easily undergo aromatic nucleophilic substitution without deactivating the substrate, thus facilitating the formation of the polymer framework. Utilizing this efficient aromatic nucleophilic substitution of thiol molecules we chose 2,3,5,6-tetrafluoroterephthaldehyde (TFTA), as a linear bridge to connect the HTT moieties into a 3D-connected CPP, with TFTA being the source of aldehydes.

The assembly of the polymer simply involves heating a mixture of DMA, TFTA, HTT (which was freshly prepared by the deprotection of HBuTT;[14] see ESI†), together with the mild base DIPEA (see Scheme S1, ESI†) to produce a dark red solid in high yield (96.8%). To further demonstrate the simplicity of this polymerization, a model reaction between 1,2-benzenedithiol and TFTA is conducted under similar reaction conditions with high yield (88%). A single crystal structure is presented for this molecular system (Fig. S9, ESI†).

Elemental analysis of PHTT_CHO is consistent with the calculated values for C, H, N (see ESI†). Thermogravimetric analysis (TGA, Fig. S1, ESI†) reveals a stable weight region up to 300 °C, indicative of the non-volatile, and polymeric nature of the product. As expected, the peak at 1681 cm^{-1} in the IR (Fig. S2, ESI†) confirms the presence of the aldehyde moiety. In addition, solid state ^{13}C NMR of a PHTT_CHO sample confirms the polymer structure as shown in Scheme 1. As seen in Fig. S3 (ESI†), the aromatic region of the solid state ^{13}C NMR spectrum of PHTT_CHO is dominated by 3 distinct peaks (135.8, 129.2 and 123.8 ppm) corresponding to the aromatic carbon signals of the polymer backbone, the peak at 188.8 ppm is assigned to the aldehyde moieties in the PHTT_CHO framework. Significant porous character of the activated sample of PHTT_CHO was revealed in both N_2 sorption (at 77 K) and CO_2 sorption (at 273 K, see Fig. S4, ESI†) experiments. A typical type-I N_2 gas adsorption isotherm (Fig. 1A) was observed, with a Brunauer–Emmett–Teller (BET) surface area of 686 m^2 g^{-1}. QSDFT analysis on pore size distribution and pore volume indicated an average pore width of 1.03 nm and a pore volume of 0.374 cm^3 g^{-1} (Fig. S6, ESI†).

Aldehyde functionalized CPPs are rare.[15] The advantages of affixing the aldehyde functionality (*e.g.*, –CHO) onto a CPP are obvious, since this moiety offers great versatility for facile and efficient post-modification reactions even in heterogeneous conditions. Aldehydes can readily undergo both reductions (*e.g.*, to give alcohol $–CH_2OH$ or halide CH_2X functions) and oxidation to form carboxyl groups, providing a convenient entry into diverse ranges of functional derivatives. An interesting post-modification strategy, known as the silver mirror reaction, relies on Tollens' reagent, which is generally used to qualitatively detect the presence of aldehydes.

Upon stirring with a freshly prepared Tollens' reagent (see ESI†) at 50 °C for 2 hours, the PHTT_CHO powder turned from dark red to black to afford the PHTT_Ag sample (Scheme 2). The strong PXRD peaks (Fig. S10, ESI†) of the silver loaded polymer sample indicate that the Ag NPs are evenly dispersed on the polymer support. The average particle size of Ag NPs is about 10 nm in diameter calculated based on the X-ray diffraction patterns.[16] Transmission electron microscopy (TEM) measurements were conducted on both PHTT_CHO and PHTT_Ag samples. Ag NPs can be readily seen in Ag NPs loaded sample (PHTT_Ag, Fig. 2B) compared to the original dark red PHTT_CHO polymer (Fig. 2A). Scanning electron microscope (SEM) (Fig. 2C) together with the corresponding elemental map of Ag atoms (Fig. 2D) obtained by energy dispersive X-ray (EDX) technique on PHTT_Ag, supported the notion of evenly distributed Ag throughout the polymer matrix. The amount of Ag NPs was quantified by ICP elemental analysis to be 33.5 wt%. As is consistent with previous studies, where Ag NPs and their aggregates was shown to block gas access to the pores,[2] the porosity of activated PHTT_Ag is markedly suppressed, with N_2 sorption revealing a decrease in surface area to 126 m^2 g^{-1} (686 m^2 g^{-1} before Ag NPs generation; Fig. 1). Additionally, the PHTT_Ag powder is more conductive (6.3 × 10^{-5} S m^{-1}; two-probe measurement) than PHTT_CHO (4.9 × 10^{-6} S m^{-1}); the enhanced conductivity can be partly attributed to the formation of the Ag NPs, even though the polymer backbone also undergoes changes in electronic structure/properties with the pendant aldehyde groups oxidized into carboxylate units. Efforts to remove

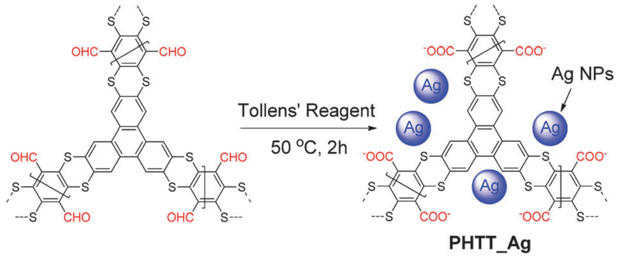

Scheme 2 The preparation of PHTT_Ag from PHTT_CHO with the *in situ* production of silver nanoparticles.

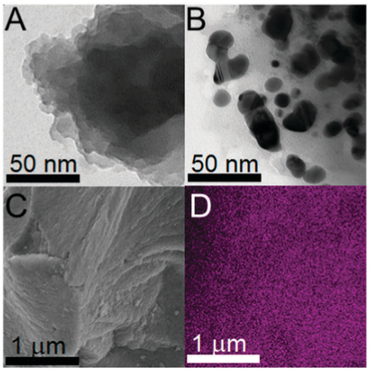

Fig. 2 TEM images of (A) PHTT_CHO, (B) PHTT_Ag, (C) SEM image of PHTT_Ag, and (D) the corresponding EDX mapping for Ag atom (purple indicates presence of Ag).

the Ag NPs from the polymer matrix are ongoing, so as to facilitate the characterization of such changes on the polymer backbone.

Nanoparticles of noble metals such as silver are very important due to their applications in catalysis.[17] Polymeric materials that support silver nanoparticles whilst retaining catalytic activity present distinct advantages over homogeneous systems, with regards ease of separation, recovery and reusability.

The catalytic activity of the PHTT_Ag polymer was examined under especially mild conditions for the reduction of aromatic nitro groups, by simply stirring the substrates with $NaBH_4$ (an inexpensive, bench stable, stoichiometric reductant) and the polymer (Ag/substrate molar ratio: about 5%) in ethanol at room temperature and under air (see details in ESI†). We tested the feasibility of PHTT_Ag as a catalyst for the reduction of various nitroarenes, keeping all other reaction conditions unaltered. As shown in Table 1, the catalyst PHTT_Ag was found to be very effective toward the reduction of nitro compounds to their corresponding anilines, regardless of the types and position of the substituents. Two control experiments were performed: (i) in the absence of PHTT_Ag there was no conversion of nitroaromatic compounds into amines; (ii) a freshly prepared silver mirror with benzaldehyde showed reduced activity in the reduction of nitrobenzene when compared to PHTT_Ag using similar conditions (followed by TLC). In particular, this reaction also showed high efficiency for the selective reduction of nitro groups in the presence of other reducible functional groups (*e.g.* alkenes, entry 6–8). The recyclability of the PHTT_Ag solid was also investigated.

Table 1 Efficiencies of the PHTT_Ag catalyst in the reduction of various nitroaromatics into amines[a]

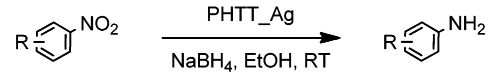

Entry	Substrate	Product	Time (h)	Conversion[b] (%)
1	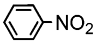	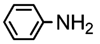	6	96
2	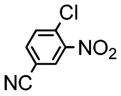	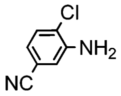	6	80
3	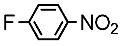	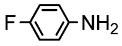	6	99
4	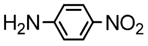	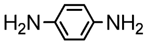	6	99
5	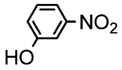	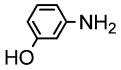	12	84
6	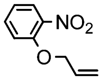	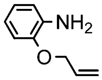	6	97
7	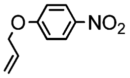	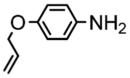	12	93
8 Cycle1	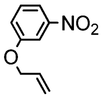	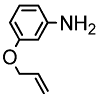	12	96
9 Cycle2[c]	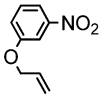	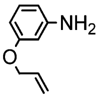	12	95
10 Cycle3[c]	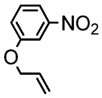	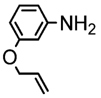	12	96

[a] Reaction conditions: substrate (0.084 mmol), $NaBH_4$ (0.672 mmol) and PHTT_Ag (1.4 mg, Ag/substrate molar ratio: 5%) in 0.5 mL ethanol at RT. [b] Conversion is determined *via* ^1H NMR using 1,2,4,5-tetramethylbenzene as the internal standard. [c] See ESI for the cycling procedure.

After the hydrogenation reaction, the catalyst can be conveniently recovered from the reaction mixture by centrifugation and subsequent washing with water and absolute ethanol. The reusability of the hybrid material was then tested after recovery. We observed no activity loss for the conversion of 1-allyloxy-3-nitrobenzene into 3-allyloxyaniline (entry 8 in Table 1). In fact, the conversion remained almost the same after 3 catalytic cycles, Fig. S13 (ESI†). Furthermore, the isolated supernatant exhibited no catalytic activity under similar reaction conditions (as verified by the NMR data in Fig. S14, ESI†), which indicates that Ag NPs were not present in the reaction mixture proving that PHTT_Ag does not leach Ag NPs under the conditions tested. This was also confirmed *via* ICP measurements where the amount of Ag within PHTT_Ag was found to be 33.4 wt% after the catalytic reactions, very close to the 33.5 wt% measured for PHTT_Ag prior to catalysis. Further cycling of the PHTT_Ag also showed no loss in activity (followed *via* TLC). However, PXRD experiments (Fig. S15, ESI†) at the 5th catalytic cycle started to reveal peaks of AgCl, which could have arisen from the Ag nanoparticles reacting with the residual NaCl trapped within the porous CPP during the earlier steps of synthesis (Scheme S1, ESI†). Apart from the ease of recovery generally associated with polymer supports, catalyst recycling in the present case can also be attributed to the anionic form of the carboxylate units in the PHTT_Ag composite (as a result of the alkaline conditions of aldehyde oxidation) – *i.e.*, the carboxylate anion minimizes the acid–base interaction with the (alkaline) amine products, and therefore facilitates their release from the polymer surface.

To sum up, several major advantages of stability and functionality have been demonstrated for this aldehyde-equipped CPP system that is conveniently produced using a metal-free strategy under mild reaction conditions. The stability is highlighted by the aqueous, alkaline and oxidative conditions in the silver mirror reaction procedure, conditions that would readily destroy MOFs, COFs and other less robust porous polymers. The Ag nanoparticles produced *in situ* were found to be evenly blended with the polymer matrix, offering highly efficient heterogeneous catalysis for the reduction of aromatic nitro compounds at room temperature. The selectivity and reusability of the composite catalyst also further illustrate the *in situ* generation of metal particles as a potentially wide-scope, effective method for enhancing the materials properties of polymer/metal nanoparticle hybrids.

This work was supported by City University of Hong Kong (Project 9667092), the Research Grants Council of HKSAR (GRF Project 103413) and the National Natural Science Foundation of China (21471037, 21201042). The X-ray diffractometer at YSU was funded by NSF Grant 1337296. We thank Mr Yan Lung Wong for drawing Fig. S9 (ESI†).

Notes and references

1 (*a*) F. Su, C. L. Bray, B. Tan and A. I. Cooper, *Adv. Mater.*, 2008, **20**, 2663; (*b*) J.-Y. Lee, C. D. Wood, D. Bradshaw, M. J. Rosseinsky and A. I. Cooper, *Chem. Commun.*, 2006, 2670; (*c*) C. D. Wood, B. Tan, A. Trewin, H. Niu, D. Bradshaw, M. J. Rosseinsky, Y. Z. Khimyak, N. L. Campbell, R. Kirk, E. Stöckel and A. I. Cooper, *Chem. Mater.*, 2007, **19**, 2034; (*d*) N. B. McKeown, P. M. Budd, K. J. Msayib, B. S. Ghanem, H. J. Kingston, C. E. Tattershall, S. Makhseed, K. J. Reynolds and D. Fritsch, *Chem. – Eur. J.*, 2005, **11**, 2610; (*e*) C. D. Wood, B. Tan, A. Trewin, F. Su, M. J. Rosseinsky, D. Bradshaw, Y. Sun, L. Zhou and A. I. Cooper, *Adv. Mater.*, 2008, **20**, 1916; (*f*) J. Germain, F. Svec and J. M. J. Fréchet, *Chem. Mater.*, 2008, **20**, 7069.

2 J. Liu, K.-K. Yee, K. K.-W. Lo, K. Y. Zhang, W.-P. To, C.-M. Che and Z. Xu, *J. Am. Chem. Soc.*, 2014, **136**, 2818.

3 F. Goettmann, A. Fischer, M. Antonietti and A. Thomas, *Angew. Chem., Int. Ed.*, 2006, **45**, 4467.

4 (*a*) H. Urakami, K. Zhang and F. Vilela, *Chem. Commun.*, 2013, **49**, 2353; (*b*) K. Zhang, D. Kopetzki, P. H. Seeberger, M. Antonietti and F. Vilela, *Angew. Chem., Int. Ed.*, 2013, **52**, 1432; (*c*) K. Zhang, Z. Vobecka, K. Tauer, M. Antonietti and F. Vilela, *Chem. Commun.*, 2013, **49**, 11158; (*d*) D. Zheng, C. Pang, Y. Liu and X. Wang, *Chem. Commun.*, 2015, **51**, 9706; (*e*) J. Zhang, M. Zhang, C. Yang and X. Wang, *Adv. Mater.*, 2014, **26**, 4121; (*f*) G. Zhang, M. Zhang, X. Ye, X. Qiu, S. Lin and X. Wang, *Adv. Mater.*, 2014, **26**, 805; (*g*) Y. Cui, Z. Ding, X. Fu and X. Wang, *Angew. Chem., Int. Ed.*, 2012, **51**, 11814; (*h*) Z. Lin and X. Wang, *Angew. Chem., Int. Ed.*, 2013, **52**, 1735; (*i*) X. Wang, K. Maeda, A. Thomas, K. Takanabe, G. Xin, J. M. Carlsson, K. Domen and M. Antonietti, *Nat. Mater.*, 2009, **8**, 76; (*j*) J. Sun, J. Zhang, M. Zhang, M. Antonietti, X. Fu and X. Wang, *Nat. Commun.*, 2012, 1139.

5 (*a*) R. Palkovits, M. Antonietti, P. Kuhn, A. Thomas and F. Schüth, *Angew. Chem., Int. Ed.*, 2009, **48**, 6909; (*b*) P. M. Budd, B. Ghanem, K. Msayib, N. B. McKeown and C. Tattershall, *J. Mater. Chem.*, 2003, **13**, 2721.

6 Z. J. Wang, S. Ghasimi, K. Landfester and K. A. I. Zhang, *Chem. Mater.*, 2015, **27**, 1921.

7 (*a*) X.-H. Li, M. Baar, S. Blechert and M. Antonietti, *Sci. Rep.*, 2013, **3**, 1743; (*b*) X.-H. Li, X. Wang and M. Antonietti, *Chem. Sci.*, 2012, **3**, 2170.

8 S. Rifai, C. A. Breen, D. J. Solis and T. M. Swager, *Chem. Mater.*, 2006, **18**, 21.

9 (*a*) H.-U. Blaser, H. Steiner and M. Studer, *ChemCatChem*, 2009, **1**, 210; (*b*) J. P. Adams and J. R. Paterson, *J. Chem. Soc., Perkin Trans. 1*, 2000, 3695.

10 L. Chen, Y. Honsho, S. Seki and D. Jiang, *J. Am. Chem. Soc.*, 2010, **132**, 6742.

11 (*a*) J.-X. Jiang, F. Su, A. Trewin, C. D. Wood, H. Niu, J. T. A. Jones, Y. Z. Khimyak and A. I. Cooper, *J. Am. Chem. Soc.*, 2008, **130**, 7710; (*b*) J.-X. Jiang, F. Su, A. Trewin, C. D. Wood, N. L. Campbell, H. Niu, C. Dickinson, A. Y. Ganin, M. J. Rosseinsky, Y. Z. Khimyak and A. I. Cooper, *Angew. Chem., Int. Ed.*, 2007, **46**, 8574.

12 (*a*) J. Schmidt, M. Werner and A. Thomas, *Macromolecules*, 2009, **42**, 4426; (*b*) J.-X. Jiang, F. Su, H. Niu, C. D. Wood, N. L. Campbell, Y. Z. Khimyak and A. I. Cooper, *Chem. Commun.*, 2008, 486.

13 J. Schmidt, J. Weber, J. D. Epping, M. Antonietti and A. Thomas, *Adv. Mater.*, 2009, **21**, 702.

14 J. Cui and Z. Xu, *Chem. Commun.*, 2014, **50**, 3986.

15 V. Guillerm, L. J. Weselinski, M. Alkordi, M. I. H. Mohideen, Y. Belmabkhout, A. J. Cairns and M. Eddaoudi, *Chem. Commun.*, 2014, **50**, 1937.

16 H. Borchert, E. V. Shevchenko, A. Robert, I. Mekis, A. Kornowski, G. Grübel and H. Weller, *Langmuir*, 2005, **21**, 1931.

17 (*a*) H. Cong, C. F. Becker, S. J. Elliott, M. W. Grinstaff and J. A. Porco, *J. Am. Chem. Soc.*, 2010, **132**, 7514; (*b*) N. Pradhan, A. Pal and T. Pal, *Colloids Surf., A*, 2002, **196**, 247; (*c*) B. Baruah, G. J. Gabriel, M. J. Akbashev and M. E. Booher, *Langmuir*, 2013, **29**, 4225.